JOURNAL OF AGRICULTURAL AND FOOD CHEMISTRY

Article

pubs.acs.org/JAFC

Engineered Nanoparticle Adhesion and Removal from Tomato Surfaces

Mahmoudreza Ovissipour,[†] Shyam S. Sablani,*[,‡] and Barbara Rasco[†]

[†]School of Food Science, Washington State University, Pullman, Washington 99164, United States

[‡]Biological Systems Engineering, Washington State University, Pullman, Washington 99164-6120, United States

ABSTRACT: Engineered nanoparticles (NPs) are being used in different industries due to their unique physicochemical properties. NPs may be toxic and could pose both public health and environmental contamination risks. In this study, two concentrations (50 and 500 μg mL^{-1}) of titania (TiO_2), silica (SiO_2), and alumina (Al_2O_3) were applied to contaminate the surface of cherry tomato as a food model, followed by washing with deionized water (DI) to remove the NPs from the tomato surfaces. The NP surface charge and hydrodynamic diameter results showed that the isoelectric point (IEP) for alumina was at pH 9−9.6, for silica at pH <3, and for titania was at pH 6.5−6.8; in addition, the highest hydrodynamic size for all NPs was observed at the IEP. Inductively coupled plasma mass spectrometry (ICP-MS) indicated that the highest NP concentration was observed on tomato surfaces contaminated at the higher concentration (500 μg mL^{-1}) ($P < 0.05$). After the tomatoes had been washed with DI, alumina levels decreased significantly, whereas for titania and silica, no significant difference in NP concentration on tomato surface was observed following the washing treatment. This study shows that removal of NPs may be possible with a simple washing treatment but that removal of NPs is likely to be more effective when the moment ratio is >1, which can occur if the pH of the washing solution is significantly different from the IEP of NPs.

KEYWORDS: *FT-IR, ICP-MS, metal oxides, nondestructive removal, SEM*

INTRODUCTION

Due to their unique physicochemical properties, engineered nanoparticles are now being used for numerous applications in the automotive, electronics, packaging polymer, pharmaceutical, and medical industries.[1,2] Nanoparticles are utilized for drug delivery, cancer therapy, bone tissue engineering, orthopedic implants, antibacterial agents, gene delivery, medical imaging, and cosmetics (antiaging cream).[2−5] Because of their widespread use, these nanoparticles (NPs) inevitably escape into the environment during manufacture, transportation, use, and disposal, ultimately contaminating soil, water, and air. The implications of NP exposure on human health and in the environment are still being examined.

Most NPs have a negative surface charge and can bind to biomolecules, especially in the gut, which may exacerbate a number of diseases.[6,7] Exposure of cells or animals to carbon nanotubes, titania (TiO_2) particles, silver nanoparticles, silica (SiO_2), and alumina (Al_2O_3) can induce cytotoxicity, gynotoxicity, and inflammation.[8−13] The toxicity of NPs depends upon different physicochemical properties such as size, distribution, state of dispersion, shape, agglomeration and aggregation, surface chemistry, surface charge, interaction with other chemicals in aqueous media, concentration, and porosity.[4,14,15]

Food could be a vehicle for NP exposure, and common items such as fresh produce are likely to be exposed to engineered nanoparticles from different forms of environmental exposure. The contact of fruits and vegetables with environmentally dispersed nanoparticles or nanoparticle-containing surfaces during cultivation, harvesting, preparation, processing, and packaging may lead to the incorporation of NPs into foods. Exposure to nanoparticles released into the air, water, and soil from consumer and industrial products could also cause food contamination. The adhesive strength of nanoparticles to cells of food plants will likely affect plant respiration during postharvest storage and potentially food quality through the generation of active oxygen species. Unfortunately, little research highlighting the detection, characterization, and quantification of engineered nanoparticles in food has been published, making it difficult to conduct adequate risk assessments at this time.[16−19] In one study the contamination of silver nanoparticles onto fresh pears was investigated[19] using a combination of techniques, including transmission electron microscopy (TEM), scanning electron microscopy (SEM), energy dispersive spectrometer (EDS), and inductively coupled plasma optical emission spectrometry (ICP-OES), for the detection, characterization, and quantification of nanoparticles, indicating that spectroscopic and microscopic techniques may be suitable analytical methods for NPs at least for some food items.[19]

Removal of NPs from contaminated surfaces remains a challenge. The physicochemical properties of NPs make their removal from silicon and organic surfaces difficalt.[20,21] Current removal methods include plasma etching, liquid etching, gas cleaning, brush cleaning, laser shock cleaning, nanobubbles, and megasonics cleaning, which have been applied in the semiconductor industry[20−23] and provide an indication of the type and severity of physical treatments that may be needed to reduce food contamination. Nanoparticle removal from any surface would depend upon particle size, surface charge, repulsive force, van der Waals force, adhesion force, surface chemical and

Received: April 26, 2013
Revised: September 26, 2013
Accepted: September 30, 2013
Published: September 30, 2013

dx.doi.org/10.1021/jf4018228 | J. Agric. Food Chem. 2013, 61, 10183−10190

physical properties, removal method, velocity of removing agent, and cleaning time. According to Bakhtari et al.,[21] particles can be removed from surfaces when the moment ratio (MR) is >1. The MR is defined by eq 1

$$\mathrm{MR} = \frac{F_d(1.74R - \Delta) + F_{dl} \times a}{F_a \times a} \quad (1)$$

where Δ is the deformation height of the particle, a is the contact radius between the deformed particle and the surface, F_d is the drag force, F_{dl} is the double-layer force, and F_a is the adhesion force.[21] Theoretically, when the removal moment overcomes the adhesion moment, the particle is removed by rolling. The drag moment acting on the particle will cause the particle to roll and detach from the surface. Increasing the repulsive force increases the zeta potential and moment ratio and decreases the van der Waals force, resulting in efficient nanoparticle removal from the surface.

In the current study, cherry tomato was selected as a model surface to investigate NP adhesion and removal. The tomato is one of the most important vegetables consumed in the United States, with an annual production of 1,379,190 tons, of which >70% is produced in California.[24] More importantly, in the fresh state, tomato is most commonly consumed without the skin being removed. Our study investigates the adhesion mechanism of NPs on tomato surfaces and whether subsequent removal of three different NPs is possible using deionized water. We selected three common metal oxide nanoparticles, alumina (Al_2O_3), titania (TiO_2), and silica (SiO_2), for this study. Detection of NPs by inductively coupled plasma-mass spectrometry (ICP-MS), SEM, and image processing was employed. Spectral changes in the biochemical properties of the tomato surface before and after treatment with a suspension of NPs was determined by Fourier transform infrared (FT-IR) spectrometry selected as an easy to use method to screen washing methods for NP removal effectiveness.

MATERIALS AND METHODS

Sample Preparation. Packaged fresh cherry tomatoes (wet weight, 8.22 ± 0.96 g; height, 30.0 ± 1.9 mm; width, 20.3 ± 0.3 mm) were purchased from a local retailer in Pullman, WA, in August 2012 and transferred to the Food Engineering Laboratory in the School of Food Sciences at Washington State University. The tomatoes were stored at 4 °C and used within 1 day. All tomatoes were washed four times using deionized water (DI) to remove particles from the surface and dried under a hood for 30 min at 20 °C. (The weight of samples remained constant.) Deionized water was provided by filtering the water through ion-exchange resin cartridge filters (APS Water Service Co., Van Nuys, CA, USA) with a pH of 5.3. Different NPs were used: Al_2O_3 (gamma, 20 nm, 99%), TiO_2 (anatase, 10−25 nm, 99%), and SiO_2 (amorphous, 20−30 nm, 99%), purchased from US Research Nanomaterials, Inc. (Houston, TX, USA). NPs were separately applied to tomato surfaces at concentrations of 50 and 500 μg mL^{-1} in deionized water at pH 4. The solution pH 4 was selected to minimize the agglomeration of nanoparticles and to obtain greater colloidal stability. After the NPs were added to deionized water in a beaker, the beakers were placed in an ultrasound bath (100 W, 40 kHz, Bransonic, Process Equipment and Supply, Inc., Cleveland, OH, USA) for 3 h to disperse the NPs. Then cherry tomatoes (two in each of three beakers; $n = 6$ for each NP) were added to the solutions for 15 min at 20 °C. Next, tomatoes were removed using forceps and dried under a hood for 30 min. The weight of sample after removal of extra surface water was the same as that of the untreated tomatoes. To study the effect of washing on removal of the NPs, tomatoes from each NP solution ($n = 6$) were immersed into the deionized water three times (5 s each time) and then dried under a hood for 30 min. No moisture loss occurred in the tomato samples during the treatment to remove surface water.

Scanning Electron Microscopy. Tomato skin of size 0.5 cm × 0.5 cm (0.25 cm^2) was carefully removed from each sample using a scalpel blade, avoiding touching the surface of the tomato so as to not remove adhering NPs (three samples for each NPs and three pieces of skin from each treated tomato) and examined by SEM (Hitachi S-570, Hitachi Ltd., Tokyo, Japan) using an accelerating voltage of 20 kV under low-vacuum conditions. Next, micrographs were taken at a 100× magnification. To avoid detachment of the NPs from the tomato surface, no fixative was applied.

Inductively Coupled Plasma-Mass Spectrometry. Tomato skins were analyzed for ^{47}Ti, ^{27}Al, and ^{28}Si by ICP-MS (7500cx series, Agilent Technologies, Santa Clara, CA, USA). The NP-treated tomato was held by inserting a sharp needle through it. The entire tomato skin was then removed carefully with a scalpel blade and oven-dried at 105 °C for 18 h. The moisture content of tomato was 0.9 ± 0.014 g H_2O g^{-1}. Dried tomato skin (200 mg) was digested in 5 mL of concentrated nitric acid in a microwave digestion system (Discover SP-D, CEM Corp., Matthews, NC, USA). Next, the digests were diluted to 25 mL with deionized water. ICP-MS conditions were as follows: a double-bypass quartz spray chamber and a concentric quartz nebulizer with argon was used as the carrier gas; plasma was operated at a power of 1600 W; flow conditions of the argon gas were 15 L min^{-1} plasma gas, 1 L min^{-1} auxiliary gas, 0.9 L min^{-1} nebulization gas, and 0.25 L min^{-1} makeup gas. Analytical grade standards and reference materials were used (AccuStandard, Inc., New Haven, CT, USA). All NP calibration standard curves showed high linear regression coefficients: Al, 0.9997; Ti, 0.9942; and Si, 0.9994. A blank of 5 mL of concentrated nitric acid was subjected to digestion as described above and diluted to 25 mL in deionized water. Tomato skins that were not treated with NPs served as controls. No NP loss was detected during microwave digestion prior to ICP-MS analysis.

Image Processing. NPs were quantified on tomato skin before treatment with nanoparticles, following treatment, and after washing. SEM images (0.25 cm^2) were analyzed using ImageJ software version 1.47a (National Institutes of Health, Bethesda, MD, USA). Images were converted to black (for surface of tomato) and white (NPs) using the threshold command. The grayscale ranged from 0 to 255, and the scale between 75 and 100 was selected to obtain images with NP visible on tomato skin surface. The magnification scale set for all images was 100 μm. The particle count, mean size, and ratio of the occupied area by nanoparticles were determined from the images.

Hydrodynamic Size and Surface Charge. The hydrodynamic size and surface charge (zeta potential) of NP dispersions were characterized using the ZetaSizer Nano ZS (Malvern Instruments Inc., UK), utilizing dynamic light scattering (DLS) and electrophoretic light scattering (ELS), respectively.[14,25] DLS measures the intensity of the laser light scattered from dissolved macromolecules or suspended particles. The dispersion hydrodynamic diameter is derived from the temporal evolution of the scattered light intensity using the Stokes−Einstein equation.[14] ELS measures the frequency or phase shift of an incident laser beam caused by electric field driven particle migration and is reported as the electrophoretic mobility using the Smoluchowski equation.[14,25] NPs were dispersed in solutions at different pH levels from 3 to 11. The pH was adjusted with either 0.1 M HCl or 0.1 M NaOH to attain the desired pH before addition of the NPs. The pH of the solutions was measured after addition of the NPs and following sonication. Zeta potential and size were determined through measurement of 1 mL aliquots in disposable capillary cell or polystyrene cuvettes (Malvern Instruments Inc.), with 10−15 measurements per sample (n = 3) at 25 °C.

Fourier Transform Infrared Spectroscopy. FT-IR spectra analysis was conducted using a Nicolet 380 FT-IR spectrophotometer (Thermo Electron Inc., San Jose, CA, USA), and spectra were taken between 4000 and 400 cm^{-1} using an attenuated total reflectance (ATR) cell. Three tomato skin pieces were separated from each sample (three samples per treatment and nine spectra per treatment) using a scalpel blade. These slices were then air-dried under laminar flow at 20 °C for 60 min. Next, samples were directly placed onto the diamond crystal cell for

spectral measurement. The assignments of FT-IR bands were 972 cm^{-1}, OCH_3 (polysaccharides, pectin); 1105 cm^{-1}, carbohydrates; 1155 cm^{-1}, stretching vibration for C−C for the presence of a carotenoid structure; 1456 cm^{-1}, CH_3 bending vibration (lipids and proteins); 1504 cm^{-1}, CH bending vibration from the phenyl rings; 1618 cm^{-1}, ring C—C stretch of phenyl; and 1725 cm^{-1}, C═O stretching band mode of the fatty acid ester.[26]

Statistical Analysis. Data analysis was performed using OMNIC (Thermo Electron Inc.). Data preprocessing algorithms were employed to analyze the spectral data, such as binning, smoothing, and second-derivative transformation, to make discernment of overlapped spectral features more distinctive. Binning reduces the number of data points in a spectrum by averaging n points into one. Smoothing eliminates high-frequency instrument noise by averaging neighboring data points. Second-derivative transformation separates overlapping absorption bands and removes baseline offsets.

To determine the influence of the washing treatment on removing the NPs from the surface of tomato, one-way analysis of variance (ANOVA) (Tukey's multiple test) using MINITAB software, release 14.12.0 (Minitab Inc., State College, PA, USA), was employed at a probability level of $P < 0.05$.

RESULTS AND DISCUSSION

Zeta Potential and Hydrodynamic Diameter. The surface of metal oxide nanoparticles becomes more positive as the pH is lowered through the following reaction:

$$MOH + H^+ \rightarrow MOH_2^+$$

If the pH is raised, the surface charge becomes more negative:

$$MOH + OH^- \rightarrow MO^- + H_2O$$

These relationships do not apply to silica, and the zeta potential for silica was negative over the pH range tested. The zeta potential and hydrodynamic diameter size for alumina, titania, and silica at 500 and 50 $\mu g\ mL^{-1}$ in aqueous suspension are presented in Figure 1. Titania (TiO_2) isoelectric point (IEP) is approximately 6.8 in a 500 $\mu g\ mL^{-1}$ and 6.5 for a 50 $\mu g\ mL^{-1}$ suspension. The zeta potential increased from 34 to 39 mV with this increase in NP concentration in solution at pH 3. These results are similar to those reported in other studies.[14,25,27,28] Suttiponparnit et al.[25] reported an increase in zeta potential from 29 to 38 mV as the titania concentration increased from 50 to 500 $\mu g\ mL^{-1}$, using experimental conditions and concentrations similar to those in the current study. The surface of titania in a dispersion is coated with hydroxyl groups and was neutral, with an IEP close to pH 7. At a lower pH, titania has a postitive surface charge and positive zeta potential. Conversely, at a pH higher than the IEP, there is a negative surface charge and negative zeta potential.[25,27,28]

The IEP for Al_2O_3 (alumina) was 9.6 at 500 $\mu g\ mL^{-1}$ and 9.0 at 50 $\mu g\ mL^{-1}$, similar to results of others.[28−31] For SiO_2 (silica), the IEP was probably lower than 3 at both concentrations and out of the range of pH (3−11) tested in this study. The reported range of IEP of silica is in the pH range of 1.6−3.5.[28,31] We found the zeta potential of silica to be negative, decreasing from −10 to −40 mV as the pH increased. Silica surfaces are protonated below the pH value of 2 and fully deprotonated at a pH value of 4.[32]

NP hydrodynamic size showed that solution pH affects the dispersion hydrodynamic diameter, reflecting the changing particle surface charge (Figure 1). The pH of fresh NP solution following sonication increased by 0.05−0.09 depending upon the type of NP. Significant agglomeration for the NPs tested in this study was observed near the IEP (titania, pH 6−7; alumina, pH 9) (Figure 1b), as the particle surface charge reached zero and the attractive van der Waals forces became dominant. These values

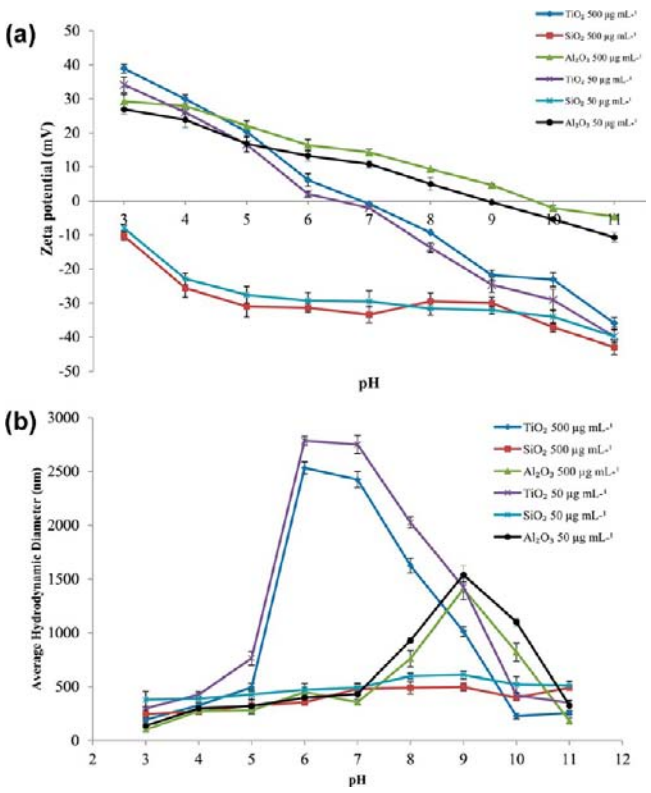

Figure 1. Influence of solution pH on the agglomeration of different NPs at two concentrations (50 and 500 $\mu g\ mL^{-1}$): (a) influence of solution pH on zeta potential; (b) influence of solution pH on hydrodynamic diameter.

are near the IEP of alumina (IEP = 9.0) and titania (IEP = 6.5). When the pH significantly differed from the IEP, as observed for titania and alumina in both concentrations, the absolute value of the zeta potential increased and the hydrodynamic size decreased. In the case of silica, a stable, clear phase was observed in water dispersions. When the repulsive energy is smaller compared to the van der Waals attraction energy, the dispersion became unstable, which gave rise to particle agglomeration. The silica nanoparticles exhibited a stable dispersion across the studied pH range and at both concentrations.[32,33] On the basis of the Derjaguin−Landau−Verwey−Overbeek (DLVO) theory, the agglomeration of nanoparticles is determined by the sum of the repulsive electrostatic force (the interaction of electrical double layer surrounding each nanoparticle) and the attractive van der Waals forces.[34,35] An increase in particle surface charge (zeta potential) can increase the electrostatic repulsive force, suppress the agglomeration, and subsequently reduce the hydrodynamic size.[25]

Characterization of NPs on Tomato Skin with SEM, Image Processing, and ICP-MS. SEM for NP-treated, washed, and control tomato skins are presented in Figure 2. No NPs were detected in the SEM images for the control group. However, the ICP-MS results (Table 2) indicated low concentrations of Al, Si, and Ti due to the presence of these minerals naturally in the plant materials. Each type of NP could be clearly observed on the surface of the tomato skin, due to backscattered electrons, which made the NPs brighter than the tomato skin. Some NPs did agglomerate on the tomato skin, and some remained in the nano size range. Similar results were reported about the agglomeration of Ag NPs (Ag) on pear tissue following treatment for 2−8 days.[19] Results of image analysis and ICP-MS show that exposing

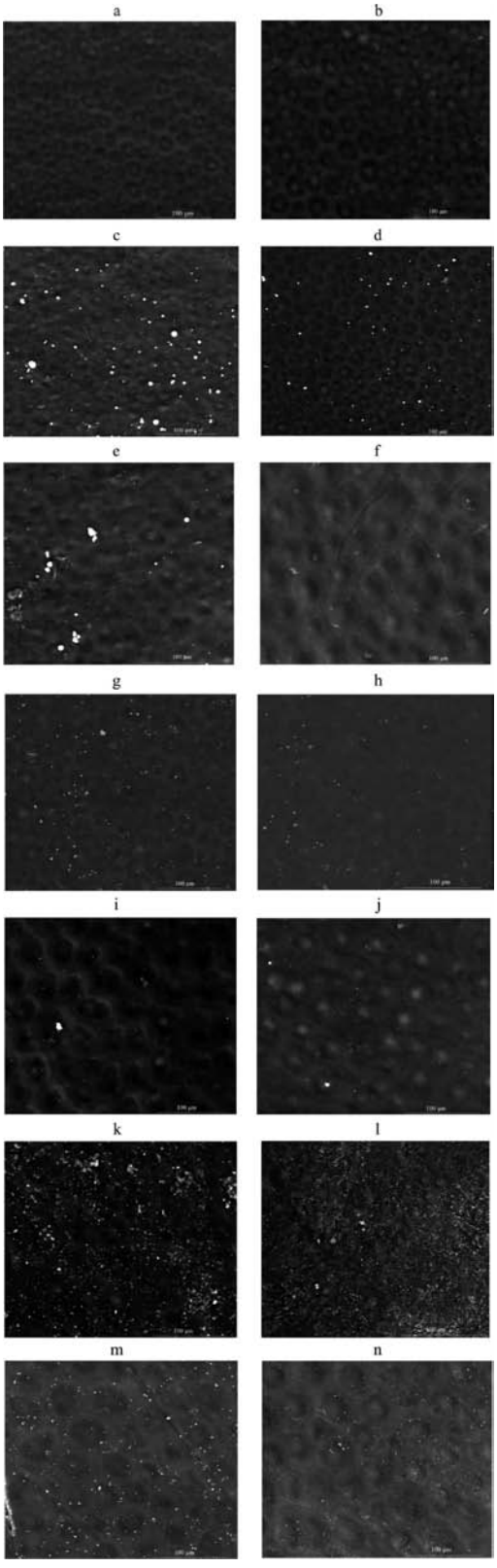

Figure 2. SEM images of tomato skin treated with different NPs: (a, b) untreated tomato skin; (c) alumina 500 μg mL^{-1}; (d) alumina 500 μg mL^{-1}, washed; (e) alumina 50 μg mL^{-1}; (f) alumina 50 μg mL^{-1}, washed; (g) silica 500 μg mL^{-1}; (h) silica 500 μg mL^{-1}, washed; (i) silica 50 μg mL^{-1}; (j) silica 50 μg mL^{-1}, washed; (k) titania 500 μg mL^{-1}; (l) titania 500 μg mL^{-1}, washed; (m) titania 50 μg mL^{-1}; (n) titania 50 μg mL^{-1}, washed.

tomato skin to higher concentrations of NPs (500 μg mL^{-1}) caused significantly more NPs to be present on the surface of the tomato for all NPs tested (Tables 1 and 2; Figure 2) ($P < 0.05$). In addition, attempts to remove NPs using a simple dip in deionized water were found to be effective for alumina (Tables 1 and 2). The number of NPs and the area (%) occupied by alumina particles significantly decreased following this DI water treatment. ICP-MS confirmed these findings, showing that the highest alumina (2.78 mg g^{-1}) was found on the tomato skin treated with the higher concentration (500 μg mL^{-1}) of alumina and that the simple DI washing treatment used decreased the alumina concentration by 87% to 0.37 mg g^{-1}. At lower concentrations (50 μg mL^{-1}), the alumina decreased by 67% from 0.33 to 0.11 mg g^{-1} tomato skin following the washing treatment. The ratio of contamination with respect to the initial concentration of alumina in the control (untreated tomato skin) showed that the deionized water can significantly decrease contamination. This effect is concentration dependent.

There are several explanations for NP adhesion onto plant surfaces, and it has been demonstrated that NPs can attach to the biological samples due to their small size.[36] In this study, NPs were dispersed in a solution with pH 4 to obtain the highest concentration of nanosized particles. NPs attach by molecular adhesion and can be adsorbed by protein, lipids, phenyl rings, etc.[37−41] FT-IR spectra showed high adhesion of NPs onto the tomato surface (Figure 4) and an effect of adhesion on spectral properties.

At higher concentrations, the alumina has a larger zeta potential and smaller size. This is because the associated increase in zeta potential (increase in repulsive force) prevented agglomeration (Figures 1 and 2). Removing NPs from surfaces depends upon the zeta potential, repulsive force, double-layer thickness, and adhesion, which can be defined as the MR (eq 1).[21] It is clear that increasing the zeta potential causes larger repulsive force, double-layer thickness, and moment ratio, which can be used to enhance NP removal.[21]

Micrographs for silica (Figure 2g−j) and titania (Figure 2k−n) indicate that a DI water wash does not completely remove these NPs from the tomato surface (Table 1). For silica, no significant difference ($P < 0.05$) was observed between contaminated and washed samples with respect to the count of NPs, the area occupied by silica (Table 1). For titania, a significantly ($P < 0.05$) higher particle count was observed in samples washed with deionized water (Table 1; Figure 2k−n). However, the overall surface area occupied by titania did not change significantly ($P > 0.05$) (Table 1), suggesting dispersion of titania particles on the tomato surface occurred after the washing treatment. In addition, the mean size of the titania particles on the surface of tomato decreased from 1.8 ± 0.53 to 0.73 ± 0.098 and 1.8 ± 0.65 to 0.15 ± 0.043 μm^2 at 500 and 50 μg mL^{-1}, respectively, also suggesting dispersion occurred. Because the overall surface area occupied by titania did not change significantly ($P > 0.05$) and only the titania average size decreased after washing, the SEM graphs related to titania could be explained. These results are confirmed with ICP-MS results, which indicated no difference between the amount of titania NPs between treated and washed tomato surfaces. ICP-MS results (Table 2) show that a high treatment concentration of NPs (500 μg mL^{-1}) resulted in significantly greater attachment of NPs onto the tomato surface, compared to the lower level (50 μg mL^{-1}). In the case of silica, the concentration of silica in the treated samples was 0.22 μg mL^{-1} at higher concentration (500 μg mL^{-1}) and 0.08 μg mL^{-1} at lower concentration (50 μg mL^{-1}), which were significantly ($P < 0.05$) higher than the

Table 1. Total Count and Area Covered by NPs on Treated and Washed Tomato Skin Using SEM and Image Analysis[a]

	alumina		silica		titania	
treatment	count	area (%)	count	area (%)	count	area (%)
exposure to 500 μg mL^{-1} aqueous suspension	501 ± 132a	3.1 ± 1.5a	1422 ± 548a	1.81 ± 0.21a	2848 ± 1105b	5.1 ± 1.9a
after three washings with deionized water, 5 s each time	216 ± 32b	0.64 ± 0.22b	1305 ± 315a	0.47 ± 0.07b	6054 ± 2390a	5.5 ± 1.8a
exposure to 50 μg mL^{-1} aqueous suspension	137 ± 25bc	0.52 ± 0.11b	342 ± 72b	0.15 ± 0.04c	273 ± 139c	0.63 ± 0.4b
after three washings with deionized water, 5 s each time	53.8 ± 35c	0.12 ± 0.05b	321 ± 44b	0.07 ± 0.04c	2515 ± 338b	1.9 ± 0.7b

[a]Values represent means ± SD (n = 9). Values in the same columns with different letters are significantly different at P = 0.05.

Table 2. Metal Concentrations on Treated and Washed Tomato Skin Using ICP-MS[a]

treatment	alumina (mg g^{-1} dry sample)	silica (mg g^{-1} dry sample)	titania (mg g^{-1} dry sample)
control	0.032 ± 0.01	0.023 ± 0.02	0.003 ± 0.0005
exposure to 500 μg mL^{-1} aqueous suspension	2.78 ± 0.43a	0.22 ± 0.02a	0.16 ± 0.019a
after three washings with DI water, 5 s each time	0.37 ± 0.14b	0.22 ± 0.02a	0.13 ± 0.007a
exposure to 50 μg mL^{-1} ENP aqueous suspension	0.33 ± 0.04b	0.08 ± 0.003b	0.02 ± 0.001b
after three washings with DI water, 5 s each time	0.11 ± 0.01b	0.08 ± 0.003b	0.02 ± 0.0002b

[a]Values represent means ± SD (n = 3). Values in same columns with different letters are significantly different at P = 0.05.

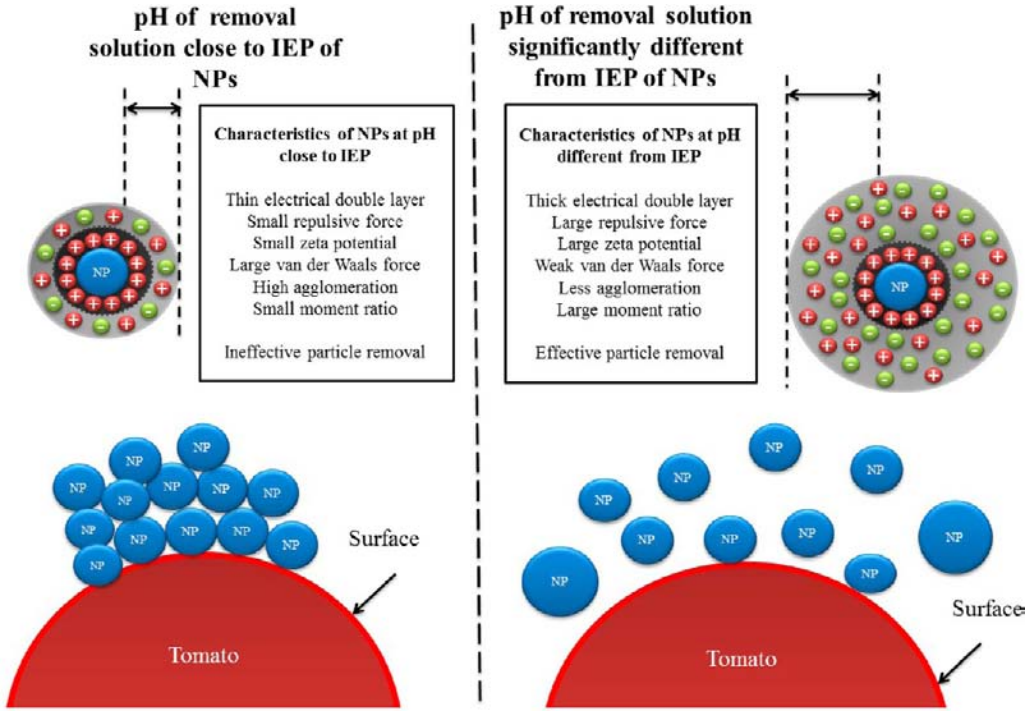

Figure 3. Interaction between NPs and tomato skin.

control group (0.023 mg g^{-1} dry sample). The quantity of titania remained constant following the washing step, whereas the particle count and area in the SEM pictures increased. This also suggests that the washing step might have dispersed titania particles.

The interaction between NPs and surfaces depends on several different parameters, including zeta potential, repulsive force, double-layer thickness, and van der Waals force (eq 1).[21] Zeta potential depends upon the pH of the colloidal suspension. Near the IEP, van der Waals forces among the NPs are dominant, resulting in a smaller double layer and lower interparticle repulsive force. Therefore, there is a lower zeta potential and ultimately high agglomeration. When the pH differs significantly from the IEP, the absolute value of the zeta potential increases, whereas the hydrodynamic size decreases. This significantly increases the ability to remove particles from a surface (Figure 3).

In this study, the pH of deionized water used to remove the NPs from tomato surfaces was 5.3, close to the IEP of titania (6.5−6.8) and within 3 pH units of the IEP of silica (1.5−3.5). The IEP of alumina (9−10) was 4 or more pH units higher, allowing for greater removal of alumina NPs compared to titania or silica. Bakhtari et al.[21] used a mixture of ammonium hydroxide, hydrogen peroxide, and deionized water (1:2:40) to remove silica nanoparticles from the surface of bare silicon wafers. They found that the mixture created a larger repulsive force between the surface and the nanoparticles, allowing for effective removal from creation of a larger MR compared to treatment with DI water.[21] In addition to the pH of the removal solution, the ionic strength of the removal solution and plant surface morphology including contact angle, surface energy, and roughness can also influence nanoparticle removal efficiency, all factors that should be investigated for developing nanoparticle removal strategy.

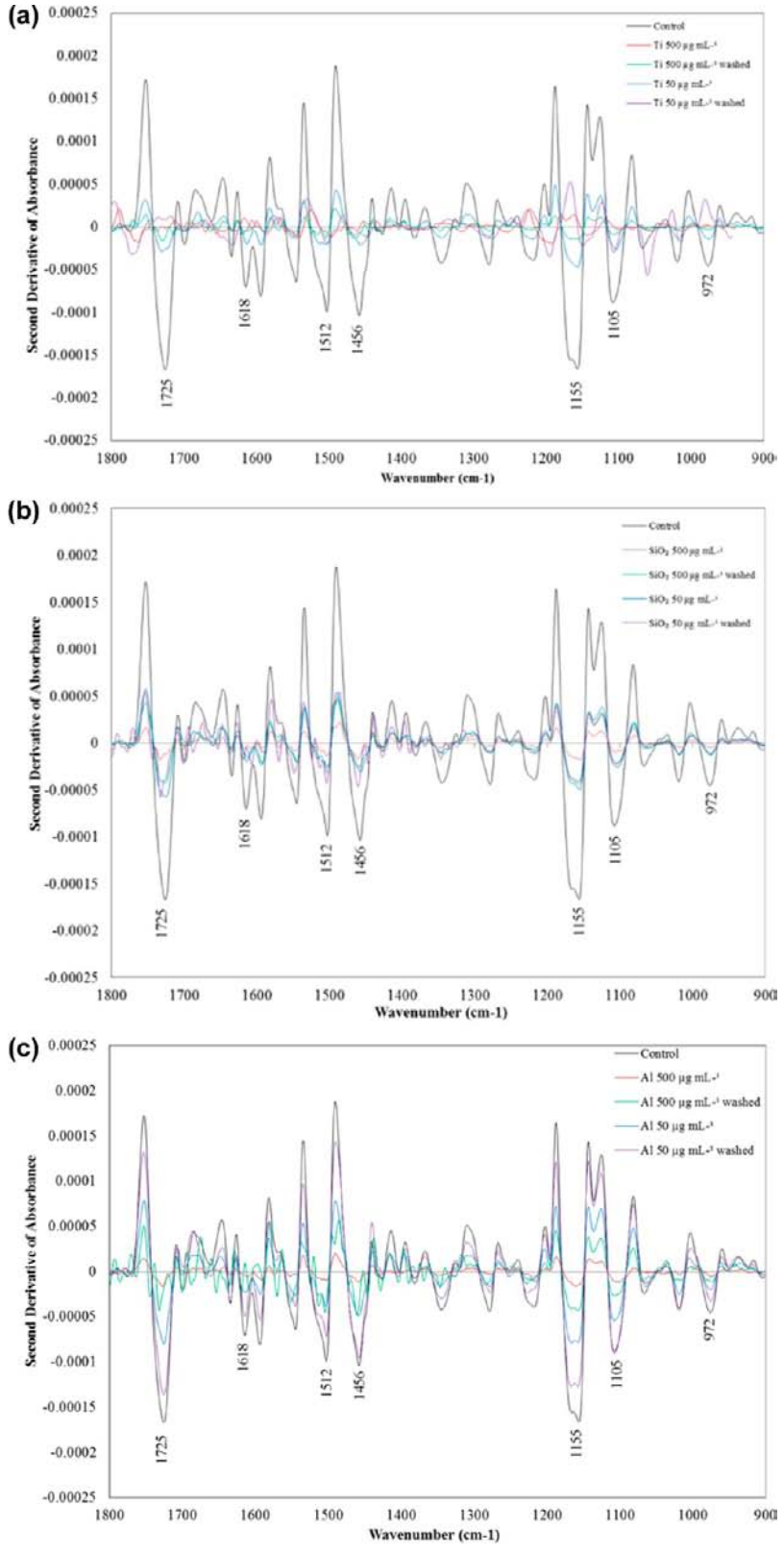

Figure 4. FT-IR spectra of untreated, NP-treated, and washed tomato skin at two different concentrations (50 and 500 μg mL^{-1}): (a) titania; (b) silica; (c) alumina.

FT-IR Spectra. Tomato surfaces were treated at two concentrations, 50 and 500 μg mL^{-1}, in deionized water at pH 4. The solution pH 4 was selected to minimize agglomeration and achieve greater colloidal stability of nanoparticles in the solution (Figure 1). Specific spectral features of biochemical components on the tomato surface were altered by the presence of NPs (Figure 4). In this study, the important spectral features affected by the presence of nanoparticles were 972 cm^{-1}, OCH_3

dx.doi.org/10.1021/jf4018228 | J. Agric. Food Chem. 2013, 61, 10183−10190

(polysaccharides, pectin); 1105 cm^{-1}, carbohydrates; 1155 cm^{-1}, stretching vibration for C—C for the presence of a carotenoid structure; 1456 cm^{-1}, CH_3 bending vibration (lipids and proteins); 1504 cm^{-1}, CH bending vibration from the phenyl rings; 1618 cm^{-1}, ring C—C stretch of phenyl; and 1725 cm^{-1}, C═O stretching band mode of the fatty acid ester. Following NP treatment, peak intensity decreased; similar results have been reported by others.[37−41] Specifically, Jankovic et al.[39] reported attachment of the titania to C−H, OH of phenyl rings, and C—C and C═C groups. The decrease in intensity depended upon the type and concentration of NPs in the treatment solution. The peak intensity changes were greater with titania compared to alumina and silica NPs. With all three NPs, the changes in band intensity observed in our study were greater at the higher NP treatment concentration (500 $\mu g\ mL^{-1}$) compared to the lower concentration (50 $\mu g\ mL^{-1}$) with the greatest effect observed for titania at the higher concentration (500 $\mu g\ mL^{-1}$). The FT-IR spectra also revealed that the washing treatment with deionized water was effective in removing alumina because initial (control) spectral features were restored at the lower NP concentration (50 $\mu g\ mL^{-1}$) with a lesser effect observed at the higher concentration of alumina nanoparticles (500 $\mu g\ mL^{-1}$), indicating that washing was less effective and NPs remained attached. However, when washing was not effective (titania and silica), no significant difference was observed in the spectral features between treated or washed tomato surfaces, confirming that NPs remained attached. These changes in FT-IR spectra further substantiate ICP-MS and SEM results (Table 2; Figure 2), showing that DI water can remove alumina but not the silica and titania NPs from tomato surfaces.

In summary, the adhesion of NPs on tomato skin increased with increasing concentration of NPs in the solution. The surface area covered by the titania NPs was greater than that by silica and alumina at the same application level (500 or 50 $\mu g\ mL^{-1}$). Washing NP-treated tomato surfaces with DI removed alumina NPs but not titania and silica. This can be explained on the basis of the difference between the pH of the removal solution (DI water, pH 5.3) and the IEP of NP. When the pH of the removal solution differs significantly from the NP IEP, the absolute value of the zeta potential of NPs increases, whereas the hydrodynamic size decreases, enhancing nanoparticle removal. The IEP of alumina (9−10) was 4 or more pH units higher than that of the removal solution, facilitating the removal of alumina NPs. The differences in the FT-IR results show that some NPs can bind to certain biochemical components such as polysaccharides and proteins on the surface of tomato skins and that when the NPs are removed, the spectral features of the native material return. A more detailed study of pH ranging from 2 to 12 and with different solutions should be made to obtain a better understanding of how nanoparticles can be removed from fruit and vegetable surfaces.

AUTHOR INFORMATION

Corresponding Author

*(S.S.S.) Phone: 1 (509) 335-7745. Fax: 1 (509) 335-2722. E-mail: ssablani@wsu.edu.

Funding

This project was supported by the College of Agriculture, Human and Natural Resource Sciences, Washington State University.

Notes

The authors declare no competing financial interest.

ACKNOWLEDGMENTS

We express our sincere thanks to Dr. Amit Bandyopadhyay, Professor, School of Mechanical and Material Engineering; Dr. Jinwen Zhang, Associate Professor, Composite Materials and Engineering Center; Dr. Valerie Lynch-Holm, specialist at the Franceschi Microscopy and Imaging Center; and Matthew Smith and Jonathan Lomber, Analytical Chemistry Service Center of the Department of Biological System Engineering, Washington State University, for useful discussion and technical support and to the Agricultural Research Center and USDA for support of this research.

REFERENCES

(1) Chen, L. Q.; Kang, B.; Ling, J. Cytotoxicity of cuprous oxide nanoparticles to fish blood cells: hemolysis and internalization. *J. Nanopart. Res.* **2013**, *15*, DOI: 10.1007/s11051-013-1507-7.

(2) Lozano, M. V.; Lollo, G.; Alonso-Nocelo, M.; Brea, J.; Vidal, A.; Torres, D.; Alonso, M. J. Polyarginine nanocapsules: a new platform for intracellular drug delivery. *J. Nanopart. Res.* **2013**, *15*, DOI: 10.1007/s11051-013-1515-7.

(3) Masciangioli, T.; Zhang, W. X. Environmental technologies at the nanoscale. *Environ. Sci. Technol.* **2003**, *37*, 102−108.

(4) Donaldson, K.; Aitken, R.; Tran, L.; Stone, V.; Duffin, R.; Forrest, G.; Alexander, A. Carbon nanotubes: a review of their properties in relation to pulmonary toxicology and workplace safety. *Toxicol. Sci.* **2006**, *92*, 5−22.

(5) Mu, Q.; Hondow, N. S.; Krzeminski, L.; Brown, A. P.; Jeuken, L. J. C.; Routledge, M. N. Mechanism of cellular uptake of genotoxic silica nanoparticles. *Part. Fibre Toxicol.* **2012**, *9*, DOI: 10.1186/1743-8977-9-29.

(6) Lomer, M. C. E.; Thompson, R. P. H.; Powell, J. J. Fine and ultrafine particles of the diet: influence on the mucosal immune response and association with Crohn's disease. *Proc. Nutr. Soc.* **2002**, *61*, 123−130.

(7) Govers, M. J. A. P.; Termont, D. S. M. L.; Aken, G. A. V.; Van der Meer, R. Characterization of the adsorption of conjugated and unconjugated bile acids to insoluble, amorphous calcium phosphate. *J. Lipid Res.* **1994**, *35*, 741−748.

(8) Geys, J.; Nemmarm, A.; Verbeken, E.; Smolders, E.; Ratoi, M.; Hoyaerts, M. F.; Nemery, B.; Hoet, P. H. Acute toxicity and prothrombotic effects of quantum dots: impact of surface charge. *Environ. Health Perspect.* **2008**, *116*, 1607−1613.

(9) Takagi, A.; Hirose, A.; Nishimura, T.; Fukumori, N.; Ogata, A.; Ohashi, N.; Kitajima, S.; Kanno, J. Induction of mesothelioma in p53± mouse by intraperitoneal application of multi-wall carbon nanotube. *J. Toxicol. Sci.* **2008**, *33*, 105−116.

(10) Chen, J.; Dong, X.; Zhao, J.; Tang, G. In vivo acute toxicity of titanium dioxide nanoparticles to mice after intraperitioneal injection. *J. Appl. Toxicol.* **2009**, *29*, 330−337.

(11) Aiso, S.; Yamazaki, K.; Umeda, Y.; Asakura, M.; Kasai, T.; Takaya, M.; Toya, T.; Koda, S.; Nagano, K.; Arito, H.; Fukushima, S. Pulmonary toxicity of intratracheally instilled multiwall carbon nanotubes in male Fischer 344 rats. *Ind. Health* **2010**, *48*, 783−795.

(12) Heng, B. C.; Zhao, X.; Xiong, S.; Ng, K. W.; Boey, F. Y.; Loo, J. S. Toxicity of zinc oxide (ZnO) nanoparticles on human bronchial epithelial cells (BEAS-2B) is accentuated by oxidative stress. *Food Chem. Toxicol.* **2010**, *48*, 1762−1766.

(13) Kocbek, P.; Teskac, K.; Kreft, M. E.; Kristl, J. Toxicological aspects of long-term treatment of keratinocytes with ZnO and TiO_2 nanoparticles. *Small* **2010**, *6*, 1908−1917.

(14) Jiang, J.; Oberdorster, G.; Biswas, P. Characterization of size, surface charge, and agglomeration state of nanoparticle dispersion for toxicological studies. *J. Nanopart. Res.* **2009**, *11*, 77−89.

(15) Freese, C.; Uboldi, C.; Gibson, M. I.; Unger, R. E.; Weksler, B. B.; Romero, I. A.; Couraud, P. O.; Kirkpatrick, C. J. Uptake and cytotoxicity of citrate-coated gold nanospheres: Comparative studies on human

endothelial and epithelial cells. *Part. Fibre Toxicol.* **2012**, *9*, DOI:10.1186/1743-8977-9-23.
(16) Gatti, A. M.; Tossini, D.; Gambarelli, A. G.; Montanari, S.; Capitani, F. Investigation of the presence of inorganic micro- and nanosized contaminants in bread and biscuits by environmental scanning electron microscopy. *Crit. Rev. Food Sci. Nutr.* **2009**, *49*, 275−282.
(17) Blasco, C.; Picó, Y. Determining nanomaterials in food. *Trends Anal. Chem.* **2011**, *30*, 84−99.
(18) Dudkiewicz, A.; Tiede, K.; Loeschner, K.; Helene, L.; Jensen, S.; Jensen, E.; Wierzbicki, R.; Boxall, A. B. A.; Molhave, K. Characterization of nanomaterials in food by electron microscopy. *Trends Anal. Chem.* **2011**, *30*, 28−43.
(19) Zhang, Z.; Kong, F.; Vardhanabhuti, B.; Mustapha, A.; Lin, M. Detection of engineered silver nanoparticle contamination in pears. *J. Agric. Food Chem.* **2012**, *60* (43), 10762−10767.
(20) Vanderwood, R.; Cetinkaya, C. Nanoparticle removal from trenches and pinholes with pulsed-laser induced plasma and shock waves. *J. Adhes. Sci. Technol.* **2003**, *17*, 129−147.
(21) Bakhtari, K.; Guldiken, R. O.; Makaram, P.; Busnaina, A.; Park, J. G. Experimental and numerical investigation of nanoparticle removal using acoustic streaming and the effect of time. *J. Electrochem. Soc.* **2006**, *153*, 846−850.
(22) Hwang, K. S.; Lee, M. J.; Yi, M. Y.; Lee, J. W. Removing 20 nm ceramic particles using a supersonic particle beam from a contoured Laval nozzle. *Thin Solid Films* **2009**, *517*, 3866−3869.
(23) Yang, S.; Duisterwinkel, A. Removal of nanoparticles from plain and patterned surfaces using nanobubbles. *Langmuir* **2011**, *27*, 11430−11435.
(24) U.S. Department of Agriculture. National Agricultural Statistics Service, 2011, http://www.nass.usda.gov (accessed Dec 25, 2012).
(25) Suttiponparint, K.; Jiang, J.; Sahu, M.; Suvachittanont, S.; Charinpanitkul, T.; Biswas, P. Role of surface area, primary particle size, and crystal phase on titanium dioxide nanoparticle dispersion properties. *Nanosci. Res. Lett.* **2011**, *6*, DOI: 10.1007/s11671-010-9772-1.
(26) Movasaghi, Z.; Rehman, S.; Rehman, I. Fourier transform infrared (FT-IR) spectroscopy of biological tissues. *Appl. Spectrosc. Rev.* **2008**, *43*, 134−179.
(27) Kosmulski, M. pH-dependent surface charging and points of zero charge III. Update. *J. Colloid Interface Sci.* **2006**, *298*, 730−741.
(28) Kosmulski, M. *Surface Charging and Points of Zero Charge*; CRC, Taylor and Francis Group: Boca Raton, FL, 2009.
(29) Pagnoux, C.; Serantoni, M.; Laucournet, R.; Chartier, T.; Baumard, J. F. Influence of the temperature on the stability if aqueous alumina suspension. *J. Eur. Ceramic Soc.* **1999**, *19*, 1935−1948.
(30) Laucournet, R.; Pagnoux, C.; Chartier, T.; Baumard, J. F. Catechol derivatives and anion adsorption onto alumina surface in aqueous media: influence on the electrokinetic properties. *Eur. Ceramic Soc.* **2001**, *21*, 869−878.
(31) Alvarez-Silva, M.; Uribe-Salas, A.; Mirnezami, M.; Finch, J. A. The point of zero charge of phyllosicicate minerals using the Mular-Roberts titration technique. *Minerals Eng.* **2010**, *23*, 383−389.
(32) Piret, F.; Su, B. L. Effect of pH and ionic strength on the self-assembly of silica colloids to opaline photonic structures. *Chem. Phys. Lett.* **2008**, *457*, 376−380.
(33) Metin, C. O.; Lake, L. W.; Miranda, C. R.; Nguyen, Q. P. Stability of aqueous silica nanoparticle dispersion. *J. Nanopart. Res.* **2011**, *13*, 839−850.
(34) Derjaguin, B. V.; Landau, L. D. Theory of the stability of strongly charged lyophobic sols and of the adhesion of strongly charged particles in solutions of electrolytes. *Acta Physicochim. URSS* **1941**, *14*, 733−762.
(35) Vewey, E. J. W.; Overbeek, J. T. G. *Theory of the Stability of Lyophobic Colloids*; Elsevier: New York, 1948.
(36) Kim, J. S.; Yoon, T. J.; Yu, K. N.; Kim, B. G.; Park, S. J.; Kim, H. W.; Lee, K. H.; Park, S. B.; Lee, J. K.; Cho, M. H. Toxicity and tissue distribution of magnetic nanoparticles in mice. *Toxicol. Sci.* **2006**, *89*, 338−347.
(37) Basu, S.; Ghosh, S. K.; Kundu, S.; Panigrahi, S.; Praharaj, S.; Pande, S.; Jana, S.; Pal, T. Biomolecule induced nanoparticle aggregation: effect of particle size on interparticle coupling. *J. Colloid Interface Sci.* **2007**, *313*, 724−734.
(38) Mihailescu, G. H.; Olenic, L.; Pruneanu, S.; Bratu, I.; Kacso, J. The effect of pH on amino acids binding to gold. *J. Optoelectron. Adv. Mater.* **2007**, *9*, 756−759.
(39) Jankovic, I. A.; Sapojic, Z. V.; Dzunuzovic, E. S.; Nedeljkovic, J. M. New hybrid properties of TiO_2 nanoparticles surface modified with catecholate type ligands. *Nanosci. Res. Lett.* **2010**, *5*, 81−88.
(40) Bian, S. W.; Mudunkotuwa, I. A.; Rpasinghe, T.; Grassian, V. H. Aggregation and dissolution of 4 nm ZnO nanoparticles in aqueous environments: influence of pH, ionic strength, size, and adsorption of humic acid. *Langmuir* **2011**, *27*, 6059−6068.
(41) Singh, A. V.; Vyas, V.; Patil, R.; Sharma, V.; Scopelliti, P. E.; Bongiorno, G.; Podesta, A.; Lenardi, C.; Gade, W. N.; Milani, P. Quantitative characterization of the influence of the nanoscale morphology of nanostructured surfaces on bacterial adhesion and biofilm formation. *PLoS One* **2011**, *6* (9), DOI: 10.1371/journal.-pone.0025029.